

Exploring the potential of nanotechnology for sustainable wood preservation

Doğu Ramazanoğlu^{a,b,*}, Ferhat Özdemir^c

Abstract: Wood preservation plays a vital role in maintaining wood products' structural and aesthetic properties. Traditional methods, including chemical treatments, preservatives, and coatings, have been utilized for wood protection, but sustainable alternatives are sought due to their negative environmental and health impacts. The utilization of nanomaterials presents a promising avenue for wood protection. In this study, nanoparticles were applied to lignocellulosic materials using the impregnation method to enhance solid wood's water and fire resistance without needing additional energy. This research aimed to identify a cost-effective and energy-efficient approach for large-scale wood production while introducing innovative and competitive materials in the wood industry. Surface modification and characterization analyses, including SEM-EDX and Optical Profilometer studies, TGA-DTA analysis for thermal strength assessment, % water uptake test for water resistance evaluation, and PCE-CSM 10 spectrophotometer measurements to determine color change parameters, were conducted. Functionalized wood surfaces treated with zinc oxide (ZnO), chitosan (Ch), and tin dioxide (SnO₂) nanoparticles exhibited water uptake values of 64%, 71%, and 73%, respectively. Following the salinization process using TEOS, the water uptake values decreased to 58%, 59%, and 60% for the respective surfaces. Based on the TGA and DTA results, the W-ZnO-TEOS sample demonstrated superior mass protection, with a significant weight loss of 62.1% (5.717 mg) at 340-375°C and 14.4% (1.328 mg) at 381-439°C. This was followed by the W-SnO₂-TEOS sample, which exhibited a weight loss of 46.3% (7.050 mg) at 301-353°C and 15.4% (2.345 mg) at 431-469°C. The W-Ch-TEOS sample displayed a weight loss of 66.4% (8.242 mg) at 342-365°C and 18.8% (2.335 mg) at 448-476°C. Overall, the W-SnO₂-TEOS sample demonstrated the highest water resistance, while the W-ZnO-TEOS sample exhibited the most effective fire protection capabilities.

Keywords: Nanoparticles, Nanotechnology, Sustainability, Water resistance, Wood Preservation

Sürdürülebilir ahşap koruma için nanoteknoloji potansiyelinin araştırılması

Özet: Ahşabın korunması, ahşap ürünlerin yapısal ve estetik özelliklerinin muhafaza edilmesinde büyük öneme sahiptir. Geleneksel yöntemler arasında kimyasal işlemler, koruyucular ve kaplamalar yer alsa da, çevresel ve sağlık açısından olumsuz etkileri nedeniyle sürdürülebilir alternatiflere ihtiyaç duyulmaktadır. Nanomalzemelerin kullanımı, ahşap koruması için yeni potansiyeller sunmaktadır. Bu çalışmada, lignoselülozik malzemelere emprenye yöntemiyle nanopartiküller uygulanarak masif ahşabın su ve yangın direnci artırılmıştır ve bu işlem için ek enerji gereksizdir gerçekleştirilmiştir. Bu çalışmanın amacı, büyük ölçekli üretim için daha maliyet-etkin ve enerji tasarruflu bir yaklaşım belirlemek ve ahşap endüstrisinde yeni ve rekabetçi malzemeler sunmaktır. Yüzey modifikasyonu ve karakterizasyon çalışmaları, SEM-EDX ve Optik Profilometre analizleri, termal mukavemet için TGA-DTA analizi, su direnci için % su alım testi ve renk değişim parametrelerini belirlemek için PCE-CSM 10 spektrofotometre kullanılarak gerçekleştirilmiştir. Çinko oksit (ZnO), Kitosan (Ch) ve kalay dioksit (SnO₂) nanopartikülleri ile işlevselleştirilmiş ahşap yüzeyler, sırasıyla %64.0 %71.0 ve %73.0 su alma değerleri sergilemiştir. TEOS ile silanizasyon işlemi sonrasında ise su alma değerleri ilgili yüzeyler için %58.0 %59.0 ve %60.0 olarak belirlenmiştir. TGA ve DTA sonuçlarına göre, W-ZnO-TEOS numunesi en yüksek kütle korumasını göstermiş ve 340-375°C'de %62.1 (5.717 mg), 381-439°C'de ise %14.4 (1.328 mg) ağırlık kaybı yaşanmıştır. Bunu takiben, W-SnO₂-TEOS numunesi 301-353°C'de %46.3 (7,050 mg) ve 431-469°C'de %15.4 (2.345 mg) ağırlık kaybı sergilemiştir. W-Ch-TEOS numunesi ise 342-365°C'de %66.4 (8.242 mg) ve 448-476°C'de %18.8 (2.335 mg) ağırlık kaybı göstermiştir. Genel olarak, W-SnO₂-TEOS numunesi en yüksek su direncini sergilerken, W-ZnO-TEOS numunesi yangın koruması açısından en etkili olduğu belirlenmiştir.

Anahtar kelimeler: Nanopartiküller, Nanoteknoloji, Sürdürülebilirlik, Su direnci, Ahşap Koruma

1. Introduction

Wood, extensively utilized in various fields including furniture, construction, and paper manufacturing, faces challenges from insects, water, and fire, impacting its aesthetic and structural characteristics. Conventional protective approaches involving chemical treatments and coatings can have adverse consequences for the environment

and human health (Clausen et al., 2004). Consequently, the exploration of sustainable alternatives (Krishnan and Adhikari, 2014; Kim et al., 2018) becomes crucial to ensure the durability and eco-friendliness of wood-based products.

Utilizing nanotechnology presents a promising alternative for wood protection, where the application of nanoparticles and nanocomposites onto wooden surfaces (Fan et al., 2013; Fan et al., 2014) can enhance resistance

^a Fibrobeton Company R&D Center, Duzce, Türkiye

^b Düzce University, Engineering Faculty, Department of Civil Engineering, Duzce, Türkiye

^c Kahramanmaraş Sutcu Imam University, Faculty of Forestry, Department of Forest Industry Engineering, Kahramanmaraş, Türkiye

* **Corresponding author** (İletişim yazarı): doguramazanoğlu@duzce.edu.tr

✓ **Received** (Geliş tarihi): 15.02.2023, **Accepted** (Kabul tarihi): 12.06.2023



Citation (Atf): Ramazanoğlu, D., Özdemir, F., 2023. Exploring the potential of nanotechnology for sustainable wood preservation. Turkish Journal of Forestry, 24(2): 122-133. DOI: [10.18182/tjf.1251521](https://doi.org/10.18182/tjf.1251521)

against decay and various forms of damage, while simultaneously improving the mechanical properties of wood (Ojanen and Kärki, 2010; Krishnan and Adhikari, 2014; Kim et al., 2018).

Biopolymers, including chitin, chitosan, starch, gelatin, and zein, offer a promising alternative for wood coating formulations due to their commercial viability and protective effectiveness (Bulian and Graystone, 2009). A notable advantage of employing biopolymers in wood conservation and protection lies in their strong compatibility with polar adhesives. Additionally, these biopolymers exhibit enhanced biodegradability at the end of their lifecycle, and the inherently polar surface of wood exhibits favorable affinity towards protein-based or cellulose-derived biopolymers.

To overcome challenges related to the utilization of biopolymers in wood protection coatings, effective methods have been developed. These challenges include water insolubility, solubility in acid solutions, and the high viscosity of biopolymer solutions. One successful approach involves the use of ionic liquids as efficient solvent media for biopolymers, enabling improved preservation of wood surfaces and enhanced protection against UV radiation (Stasiewicz et al., 2008; Garcia et al., 2010; Croitoru et al., 2015; Patachia et al., 2012).

Chitosan, derived from crustacean shells, has shown promise as a wood preservative, either alone or as an additive in antifungal formulations, exhibiting efficacy against wood decay fungi and mold fungi (Laflamme et al., 2000; Alfredeen et al., 2004; Eikenes et al., 2005; Larnøy et al., 2005; El-Gamal et al., 2016). Studies have found that chitosan with high molecular weight demonstrates greater effectiveness against wood decay fungi, while its effectiveness against mold fungi can be enhanced by combining it with other polymers like polyethylene glycol (PEG) for improved physical and chemical stabilization on the wood surface (Eikenes et al., 2005; Reddy et al., 2012; Nowrouzi et al., 2016).

Utilizing lignin, a biopolymer extracted from wood, as a UV stabilizer in wood coating formulations presents an intriguing approach (Schaller and Rogez, 2007). The phenols released from lignin can be absorbed by treated wood surfaces, effectively acting as biocides against rot fungi (Chirkova et al., 2011). Lignin ester-based derivatives, obtained through reactions with lauroyl chloride, can serve as efficient hydrophobization agents in protective coatings for wood surfaces (Herrera et al., 2016). High-lignin-content bio-based polyurethane systems offer high-performance coatings with improved thermal stability, excellent film-forming ability, enhanced hydrophobization properties, and strong adhesion to wood surfaces (Griffini et al., 2015).

The application of ultrasonic waves induces a phenomenon known as the "sponge effect," resembling the squeezing and releasing motion of a sponge, enabling the rapid extraction of moisture from liquid-immersed materials (Ramazanoğlu and Özdemir, 2020a; 2020b; 2020c; Wan et al., 1992). This effect, coupled with the mechanical and physical impacts of ultrasound, contributes to enhanced diffusion effects (Floros and Liang, 1994). The formation of microscopic new channels within porous materials as a result of ultrasonic treatment reduces the diffusion boundary layer and promotes increased mass transfer (Tarleton, 1992; Tarleton and Wakeman, 1998; De La Fuente-Blanco et al., 2006).

Recent investigations have highlighted the significant reduction in drying time and overall acceleration of the process by employing ultrasonic baths as a pretreatment (Ramazanoğlu and Özdemir, 2020d; 2021; 2022; Duan et al., 2008; Aversa et al., 2011; Jangam, 2011; Mothibe et al., 2011). This effect is attributed to various factors, including heightened mass transfer rates (Garcia-Perez et al., 2009; Xu et al., 2009; Carcel et al., 2011; Garcia-Perez et al., 2011), improved water penetration (Bantle and Eikevik, 2011; He et al., 2012), increased wood-specific permeability coefficient (Tanaka et al., 2010), disruption of cellular adhesion, formation of wider cell gaps, rupture of cell walls, and creation of larger channels (He et al., 2012).

This study aims to increase the resistance of solid wood to water and fire by using the synergic effect of both positively charged biopolymer chitosan, ZnO, SnO₂ nanoparticles, and Tetraethyl orthosilicate (TEOS) on the wooden surface without requiring additional energy under room conditions. The goal is to provide a more realistic, cost-effective, energy-efficient, and low-labor approach that can increase the competitiveness of large-scale production and provide affordable and high-quality materials for consumers.

The findings demonstrate that incorporating nanoparticles in the impregnation process offers a partial enhancement in solid wood's resistance to water and fire at ambient conditions, without the need for additional energy. This approach holds promise as a cost-effective and sustainable solution for safeguarding wooden materials in large-scale applications. Moreover, the application of nanotechnology can improve wood's mechanical properties and prolong its lifespan, thereby increasing its appeal in the construction, furniture, and paper manufacturing sectors.

2. Materials and methods

2.1. Materials

In this study, wooden stirrers made of 100% Birchwood (originating from China) with a thickness of 1.00 mm, width of 5.00 mm, and length of 110 mm were purchased from a local market. Chitosan (Cas no: 9012-76-4), Acetic acid (CH₃COOH % 99.8-100.5 Cas no: 27225-2.5L-R), and Tetraethyl orthosilicate (TEOS) (Cas no: 86578-1L % 99.0) were purchased from Sigma ALDRICH company. TK.200650.05001 Ethyl alcohol (EtOH) 96% Teksoll Extra pure, TK.090250.05001 Isopropyl alcohol (2-Propanol), and TK.92008501002 Zinc Nitrate Hexahydrate [Zn(NO₃)₂·6H₂O] Extra pure were purchased from TEKKIM company, and Tin(II) chloride dihydrate (SnCl₂·2H₂O) was purchased from MERCK company.

2.2. Methods

Preparation of wood samples

Wood samples were washed with pure water in an ultrasonic bath (Figure 1) for 15 minutes at 25°C using an ultrasonic frequency of 40 kHz. Then, they were dried at 105±2 °C until the weight was not changed.

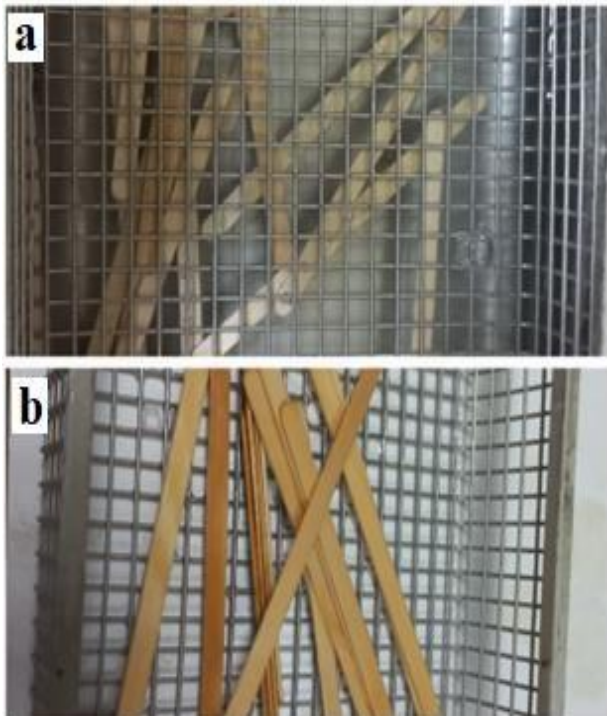


Figure 1. (a): Ultrasonic washing and (b) after.

Preparation of solutions

1 gram of chitosan (Ch) was dissolved in 200 ml of 3% acetic acid (CH_3COOH) solution (Figure 2) as shown below.

A 200 mL solution of 0.5 M Zinc Nitrate [$\text{Zn}(\text{NO}_3)_2 \cdot 6\text{H}_2\text{O}$] was prepared for application to the wooden samples, while a 200 mL solution of 0.5 M Tin (II) Chloride Dihydrate ($\text{SnCl}_2 \cdot 2\text{H}_2\text{O}$) was prepared in a mixture of water and ethanol (2:1 ratio). The preparation of the wooden surfaces and solutions is shown schematically in Figure 3.

Solutions were prepared by adjusting the pH to 2-3 using 37% hydrochloric acid (HCl) (Figure 3a) to ensure the positive charging of the nanoparticles in the solution (Zhou and Fu, 2020). Then, wooden samples with dimensions of 1.00 X 5.00 X 110 mm, which were negatively charged due to the presence of hydroxyl groups on their surfaces, were immersed in three different solutions containing positively charged particles (Figure 3b). The samples were left in the solutions for 90 minutes, during which time the positively charged particles were absorbed by the wooden samples through electrostatic forces and self-adhered to the lignocellulosic surface (Figure 4). Afterward, the wood samples were washed with distilled water and dried in an oven at 60°C for 1 hour.



Figure 2. Preparation of chitosan solution.

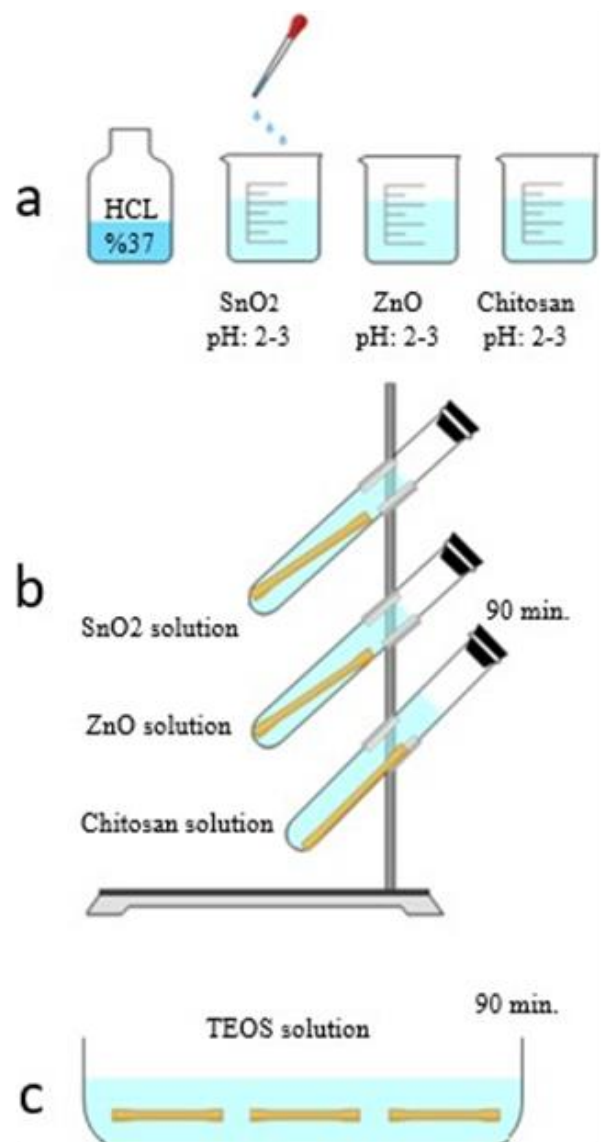


Figure 3. Schematic representation of the preparation of wooden substrate and solutions

Subsequent to treatment with tin, zinc, and chitosan solutions, wood samples were impregnated with a TEOS solution, prepared in accordance with the methodology outlined in Figure 3c (TEOS: EtOH = 1:2 V/V) for a duration of 90 minutes. Following impregnation, the wood samples were subjected to a second round of washing with distilled water. To facilitate the drying process, the samples were then placed in an oven set at $103\pm 2^{\circ}\text{C}$ for 1 hour, as depicted in Figure 5. While the weight measurements of the wood materials were conducted both before and after modification, they were not performed under any specific conditions. Notably, the samples were not subjected to conditioning in the climatic chamber.

Surface Roughness

An optical profilometer device (Phase View brand) was utilized to take surface roughness measurements, is a non-invasive approach to measuring the surface profile, height, and shape of objects (Figure 6). The method involves illuminating the object's surface with a profilometer and then measuring the amount of reflected light. This data is then utilized to generate a three-dimensional image of the surface, which can be utilized for various applications, including detecting surface defects, measuring surface heights, and determining surface roughness. Two common profile parameters used in optical profilometry are Ra, which denotes the average roughness of the surface, and Rz, which denotes the average maximum height of the profile.

Color measurements

The color analysis of the wood samples was conducted at the Fibrobeton R&D center using a PCE-CSM 10 spectrophotometer (Figure 7). The color alteration observed on the lignocellulosic surface serves as an indicator of surface functionalization. The PCE-CSM 10 spectrophotometer quantifies colors based on the CIE Lab* color space standard. This standard provides an objective definition and measurement of the lightness (L^*), the position between red/green (a^*), and the position between yellow/blue (b^*) for a specific color (ASTM-D2244-21, 2021).



Figure 5. Final dried samples obtained by treatment with TEOS.

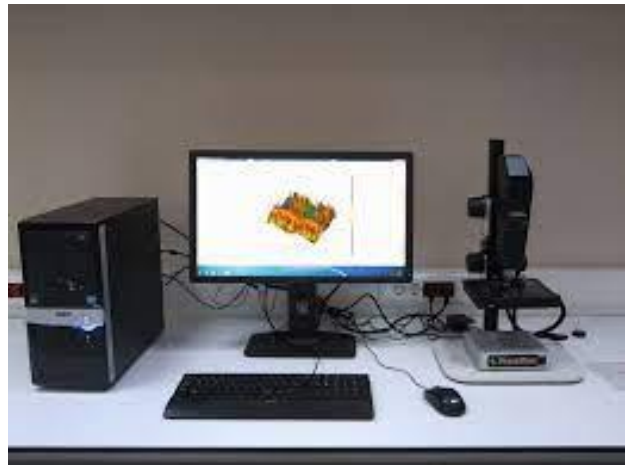


Figure 6. Optical profilometry.



Figure 4. Impregnation method.



Figure 7. PCE-CSM 10 spectrophotometer device.

Thermogravimetric Analysis

Thermogravimetric analysis (TGA) is a common analytical technique used to measure how the weight of a sample changes with temperature. It is used to study the thermal behavior of materials, such as the amount and rate of weight loss, the temperatures at which degradation or decomposition occurs, and the residue weight after processing. TGA has a wide range of applications in many fields, such as materials science, chemistry, and environmental science, to determine thermal stability, composition, purity, and contamination of materials. The technique is based on the principle that the weight of a sample changes due to physical or chemical processes (such as evaporation, oxidation, and decomposition) when heated. This study compared the thermal stabilization of wood samples functionalized with nanoparticles using the impregnation method. Thermogravimetric and differential thermal analyses (TGA/DTA) were conducted using a DTG 60H - DSC 60TGA model device from the Shimadzu brand (Figure 8).

SEM & EDX Analysis

Moreover, imaging and measurements for Scanning Electron Microscopy-Energy Dispersive X-ray Analysis (SEM-EDX) were performed using FEI brand equipment, specifically the Quanta FEG 250 model (Figure 9), at the Scientific and Technological Research Application and Research Center (DÜBİT).

Water uptake (%)

The wood samples' water uptake ratio (%) was determined by measuring their weight after being submerged in water for 24 hours (as shown in Figure 19) and applying formula (1):

$$SW = \frac{M_w - M_d}{M_d} \times 100 \quad (1)$$

Here, M_d represents the initial weight of the sample in grams, M_w is the weight of the sample after being immersed in water in grams, and SW is the water uptake ratio expressed as a percentage.



Figure 8. DTG 60H device.



Figure 9. SEM-EDX device.

3. Results and discussion

3.1. SEM & EDX Analyses

The SEM and EDX images of the massive wood (W) representing the control sample are given in Figure 10.

The carbon (C) and oxygen (O) peaks observed in the EDX spectrum in Figure 10 are attributed to the elements abundant in the main components of wood, cellulose, hemicellulose, and lignin, due to their structural properties. Since there is no coating or nano-accumulation on the wood surface, the lumens and channels are clearly visible.

Figure 11 shows the SEM image and EDX analysis of the wood surface that was impregnated with chitosan solution positively charged by adding HCl for 90 minutes.

As a result of the EDX spectrum analysis, the emergence of the nitrogen (N) peak due to the attachment of chitosan to the lignocellulosic surface was observed. The N amount of 1.31% may belong to the chitosan on the surface, and the chlorine amount of 1.03% may be attributed to the HCl acid used for pH adjustment. Additionally, it was determined that the lumens were closed due to the accumulation of chitosan on the surface (Figure 12).

When positively charged ZnO nanoparticles accumulate on the lignocellulosic surface, the EDX spectrum analysis reveals that 42.4% C, 45.8% O, and 9.76% Zn are adsorbed by the surface. Compared to the solid surface, the ZnO accumulations are observed in the SEM image to accumulate along the lumens and channels (Figure 13).

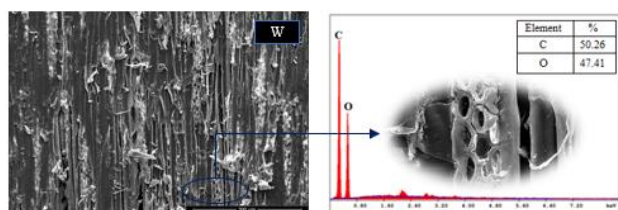


Figure 10. Elemental analyses of the massive (W) surface with SEM and EDX images.

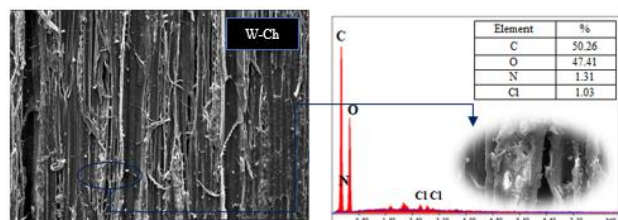


Figure 11. SEM & EDX analyses of the wood-chitosan (W-Ch) surface.

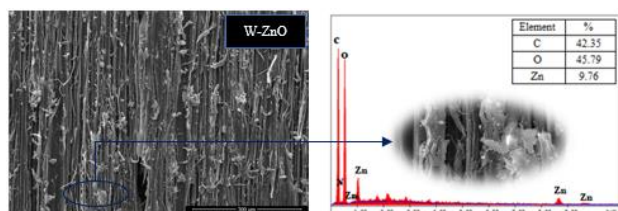


Figure 12. SEM & EDX analyses of the wood-ZnO (W-ZnO) surface

SEM and EDX analyses of the massive sample immersed in a solution containing positively charged SnO₂ particles are given in Figure 13.

According to the EDX results, it was determined that tin (Sn) particles are located on the wood surface at a rate of 25.73% due to electrostatic forces of negatively charged hydroxyl groups. In addition, the SEM images show SnO₂ particle adhesions (Figure 14).

Wood samples impregnated with positively charged chitosan solution were treated with tetraethyl orthosilicate ethanol (TEOS/EtOH) solution for 90 minutes to enhance the hydrophobization of the surface. This treatment, known as silanization, was the final step in the functionalization process. According to SEM and EDX analyses, silanization was successful, as evidenced by the appearance of peaks for 21.29% silicon (Si) and 0.26% fluorine (F) in the EDX spectrum after the treatment (Figure 14). Furthermore, the waxy layer that provides hydrophobization was observed in the SEM image after silanization. The carbon and oxygen peaks observed in the EDX spectrum were typical of lignocellulosic structures, and the presence of a 1.27% nitrogen (N) peak was due to chitosan accumulation prior to silanization (Figure 14).

It is observed that the silanization process is successful on wood surfaces impregnated with zinc and tin solutions by treating them with a Tetraethyl orthosilicate Ethanol (TEOS/EtOH) solution for 90 minutes. Silan peaks were detected at a rate of 19.86% on the surface containing ZnO particles (Figure 15), and at a rate of 33.05% on the surface covered with SnO₂ particles (Figure 16).

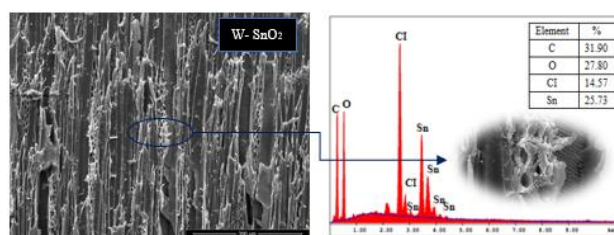


Figure 13. SEM & EDX analyses of the wood-Tin dioxide (W-SnO₂) surface

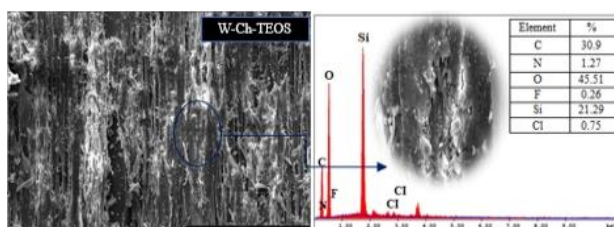


Figure 14. SEM & EDX analyses of the wood-chitosan-TEOS (W-Ch-TEOS) surface

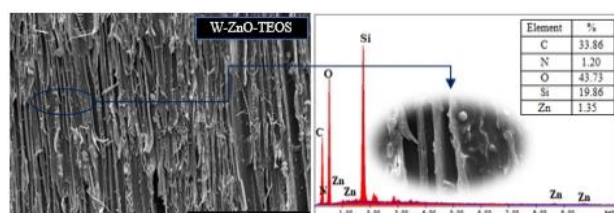


Figure 15. SEM & EDX analyses of the wood-ZnO-TEOS (W-ZnO-TEOS) surface

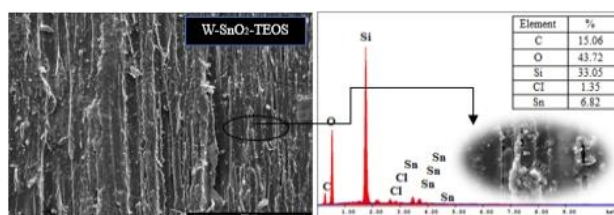


Figure 16. SEM & EDX analyses of the wood-Tin dioxide-TEOS (W-SnO₂-TEOS) surface

3.2. Color analyses

The color measurement parameters are shown in the graph in Figure 17.

The color change parameters of the wooden samples were compared to the control sample, which had L*, a*, and b* values of 78.1, 5.53, and 16.7, respectively.

In the case of the wooden surface coated with Zn particles, an increase of 3.87% was observed in the L* parameter, indicating a whiter appearance. There was also an increase of 26.8% in the a* parameter, indicating a change in red/green color tones, and a 6.34% increase in the yellow/blue color values. However, in the Zn-TEOS sample, a 4.35% decrease in the L* value, a 37.1% increase in the a* value, and a 6.22% increase in the b* values were observed.

For the wooden surface functionalized with Sn particles, the L*, a*, and b* color parameter values decreased by 9.69%, and 58.0%, and increased by 15.9%, respectively, when compared to the control sample. In the Sn-TEOS sample, the L* and a* parameters decreased by 9.77% and

7.41%, respectively. There was a 0.41% increase in the b^* color parameter of the Sn-TEOS sample.

As a result of the location of Ch particles, a 14.4% decrease was observed in the L^* value of the lignocellulosic surface compared to the control sample. It is possible to say that there was an increase of 66.0% and 20.0% in the other color parameters a^* and b^* , respectively. All color parameter values of the Ch-TEOS sample increased by 1.43%, 7.59%, and 9.88% in L^* , a^* , and b^* values, respectively, when compared to the control sample.

3.3. Optical profilometry

As profile parameters, Ra (average roughness of the surface) and Rz (average maximum height of the profile) could be used as an objective approach to evaluating surface morphology in this study. The surface parameters of the control sample (W) were measured as Ra: 0.34 μm and Rz: 1.16 μm . The surface parameter values of the W-Ch sample intervened with positively charged chitosan particles were determined as Ra: 0.25 μm and Rz: 1.05 μm . Here, it was observed that there was a 24.7% decrease in the arithmetic average roughness value Ra of the surface after impregnation with chitosan, while there was a 9.39% decrease in the mean maximum height value of the profile (Rz). When the location of zinc oxide (ZnO) particles on the wood surface was compared with the control, it was determined that the Ra value decreased by 30.3% to 0.23 μm and the Rz value

decreased by 24.8 % to 0.87 μm . Similarly, after impregnation with SnO₂ particles, the surface parameters of the W-SnO₂ sample were measured as Ra: 0.23 μm and Rz: 0.90 μm , respectively, showing a decrease of 30.5% and 22.3% (Figure 18).

The surface roughness parameters, Ra and Rz, of the W-Ch, W-ZnO, and W-SnO₂ samples, after being modified by silanization with TEOS, were determined and presented in Figure 19.

The surface roughness parameters Ra (average roughness) and Rz (average maximum height of the profile) were evaluated for W-Ch, W-ZnO, and W-SnO₂ samples after silanization with tetraethyl orthosilicate (TEOS), as shown in Figure 19. The results demonstrated that the average surface roughness value Ra of the W-Ch-TEOS sample was measured to be 0.09 μm , with an Rz value of 0.39 μm , representing a reduction of 72.8% and 22.3%, respectively, compared to the solid samples. Similarly, the surface parameters of the W-ZnO-TEOS sample were decreased by 41.0% and 30.4%, measuring 0.20 μm and 0.81 μm , respectively, compared to the control sample. In the case of W-SnO₂-TEOS, the Ra value was found to be 0.17 μm , and the Rz value was 0.68 μm , which represents a decrease of 47.6% and 41.5%, respectively, compared to control W. These findings suggest that silanization with TEOS can effectively modify the surface roughness of the wood samples.

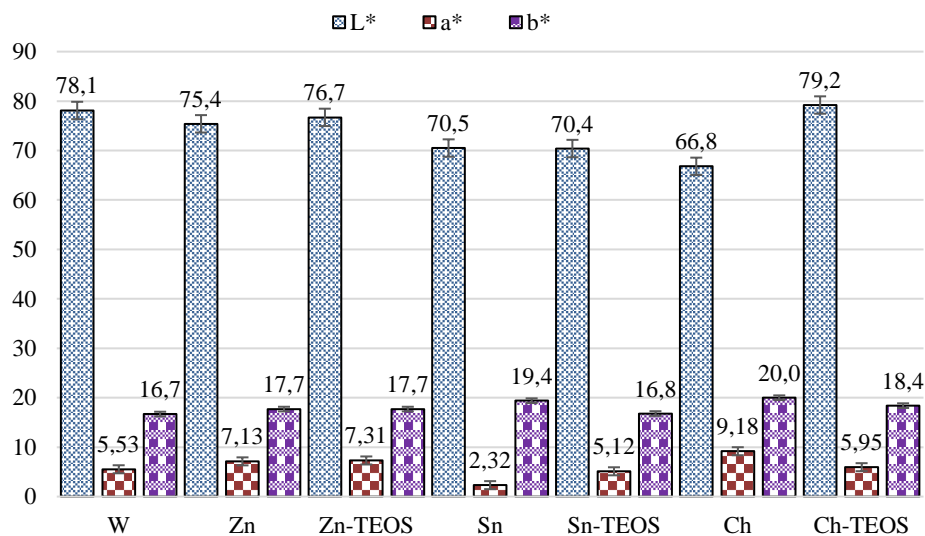


Figure 17. The color parameters (%)

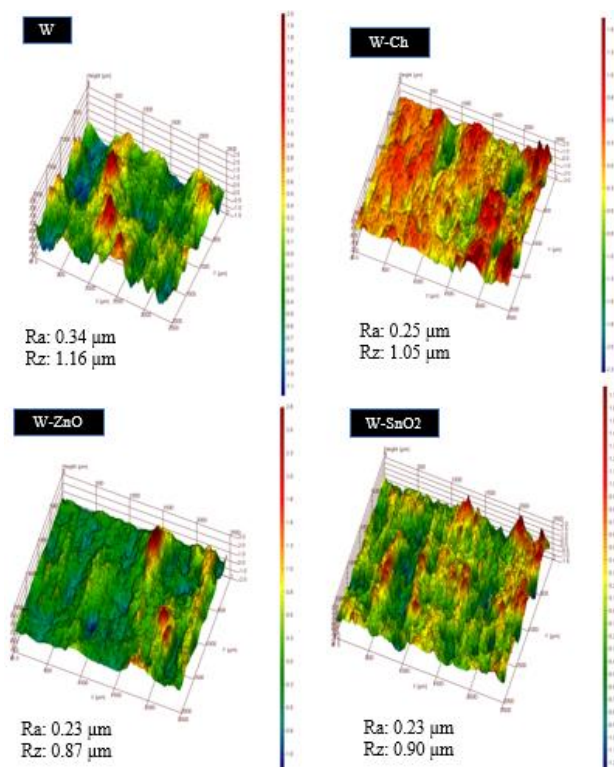


Figure 18. The measured surface roughness parameters are Ra and Rz values of W, W-Ch, W-ZnO, and W-SnO₂ samples.

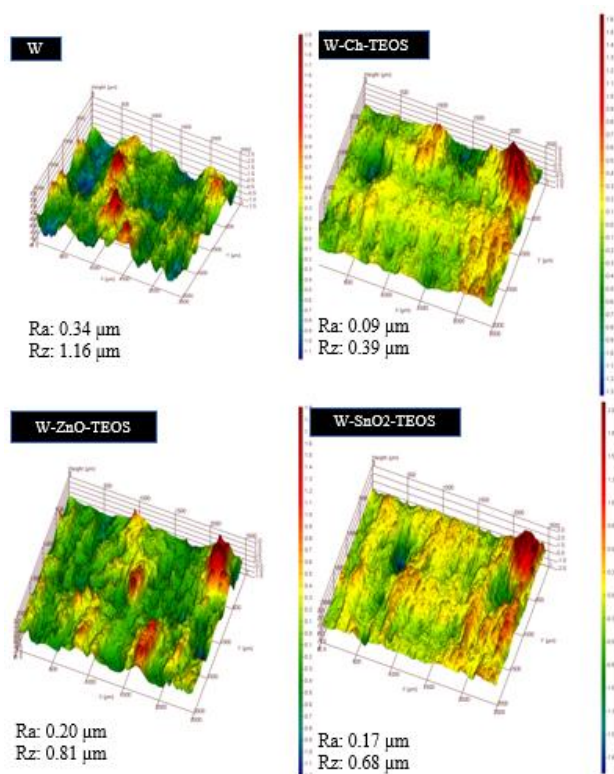


Figure 19. The surface parameters after silanization by TEOS.

3.4. Thermogravimetric analysis

TGA and DTA graphs of W, W-Ch, W-ZnO, and W-SnO₂ were given in Figures 20 and 21.

The TGA (Thermogravimetric Analysis) curves of the control (W) and functionalized W-Ch, W-ZnO, and W-SnO₂ samples exhibit similar oscillations up to 100°C. This may be attributed to the departure of water molecules from the lignocellulosic structure (Zhou et al., 2011; Ramazanoğlu and Özdemir, 2022). The control sample (W) shows a weight loss of 40.7% (2.732 mg) at 350-363°C, which could be attributed to the depolymerization of hemicellulose, and a second major decomposition peak at 458-478°C resulting in a weight loss of 16.7% (1.164 mg), likely due to cellulose degradation. Loss of hemicellulose typically occurs between 150 and 220°C, where thermal decomposition leads to the degradation of sugar components within the hemicellulose structure. Cellulose loss occurs at higher temperatures, usually starting between 200 and 300°C. Within this temperature range, the amorphous structures of cellulose break down, and smaller molecules are formed (see Figures 20, 21).

Figures 22 and 23 show the TGA and DTA graphs for solid wood (W), zinc-functionalized surface (W-ZnO), and after silanization (W-ZnO-TEOS).

In the W-Ch (wood-chitosan) sample, a significant weight loss of 72.7% (6.436 mg) was observed between 341-359°C, indicating the decomposition of certain components. Another weight loss of 18.9% (1.164 mg) was observed at 468-485°C. Following the silanization process, the W-Ch-TEOS sample exhibited a weight loss of 66.4% (8.242 mg) at 342-365°C and 18.8% (2.335 mg) at 448-476°C, suggesting the presence of functional groups other than biomass (Figure 20, 21).

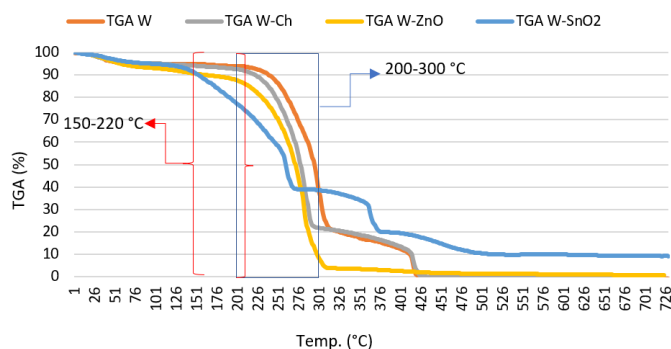


Figure 20. TGA spectra of W, W-Ch, W-ZnO, and W-SnO₂.

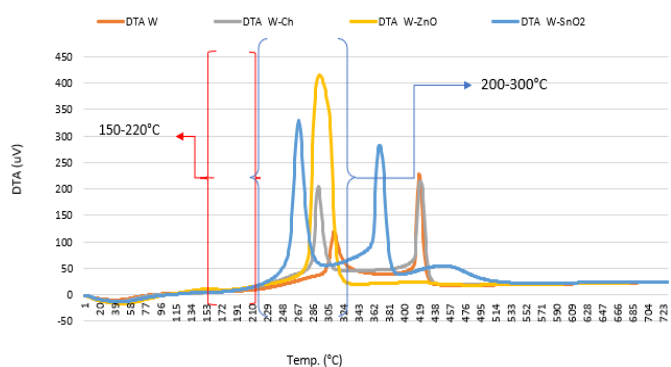


Figure 21 DTA spectra of W, W-Ch, W-ZnO, and W-SnO₂.

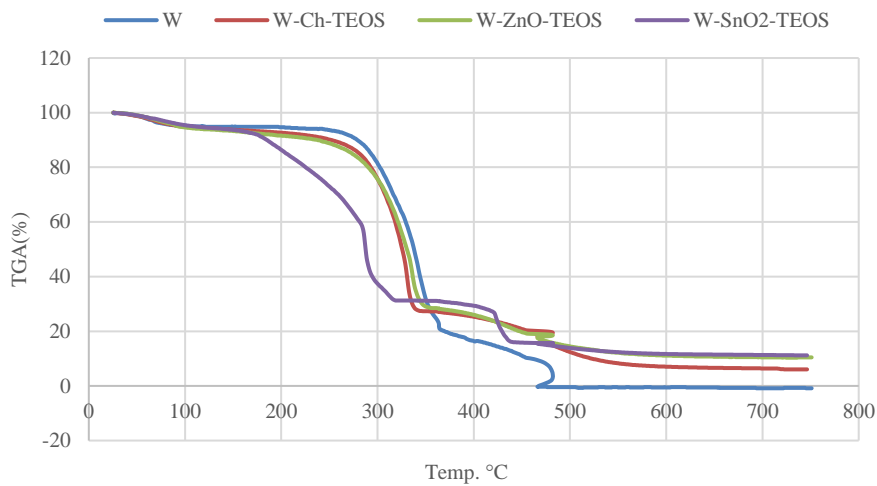


Figure 22. TGA spectra of W, (Wood), W-Ch-TEOS (Wood-Chitosan-TEOS), W-ZnO-TEOS (Wood-ZnO-TEOS), and W-SnO₂-TEOS(Wood-SnO₂-TEOS).

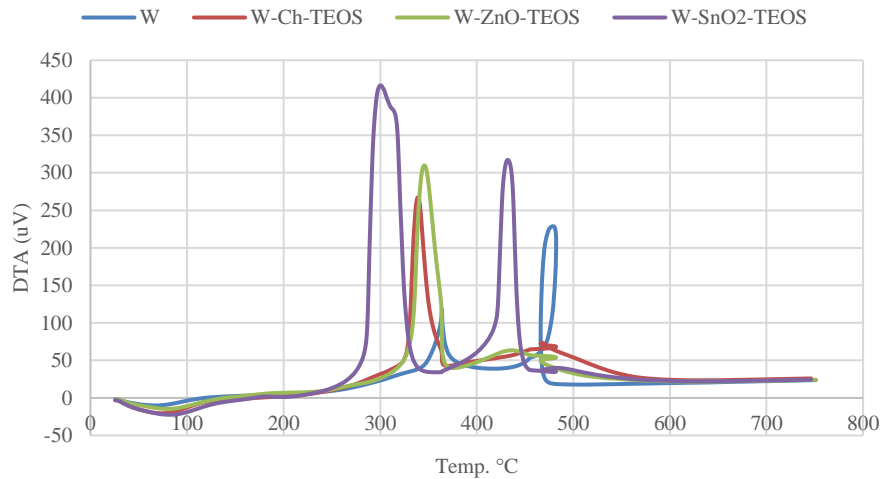


Figure 23. DTA spectra of W (Wood), W-Ch-TEOS (Wood-Chitosan-TEOS), W-ZnO-TEOS (Wood-ZnO-TEOS), and W-SnO₂-TEOS(Wood-SnO₂-TEOS).

For the W-SnO₂ (wood-tin dioxide) sample, the first weight loss occurred at 304-343°C with a rate of 31.4% (2.922 mg), indicating the decomposition of certain components. Another weight loss of 18.9% (1.763 mg) was observed at 410-437°C. Additionally, a third weight loss of 9.61% (0.894 mg) was observed at 437-490°C. After silanization with TEOS, the W-SnO₂-TEOS sample exhibited a weight loss of 46.3% (7.050 mg) at 301-353°C and 15.4% (2.345 mg) at 431-469°C.

The first weight loss was observed in the W-ZnO (wood-zinc oxide) sample at 338-387°C, accounting for 85.3% (7.957 mg) of the total weight loss. The second weight loss occurred at 365-462°C, representing a smaller proportion of 2.07% (0.193 mg). After treatment with TEOS, the first weight loss of W-ZnO-TEOS was observed at 340-375°C, accounting for 62.1% (5.717 mg) of the total weight loss. The second decomposition was observed at 381-439°C, representing 14.4% (1.328 mg) of the weight loss.

The illustration of the repelling of the new surface after silanization with TEOS is depicted in Figure 24.

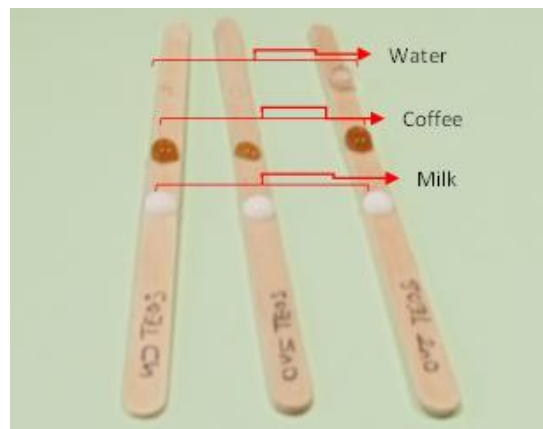


Figure 24. After silanization with TEOS the surface repellency of W-Ch-TEOS (Wood-Chitosan-TEOS), W-ZnO-TEOS (Wood-ZnO-TEOS), and W-SnO₂-TEOS (Wood-SnO₂-TEOS).

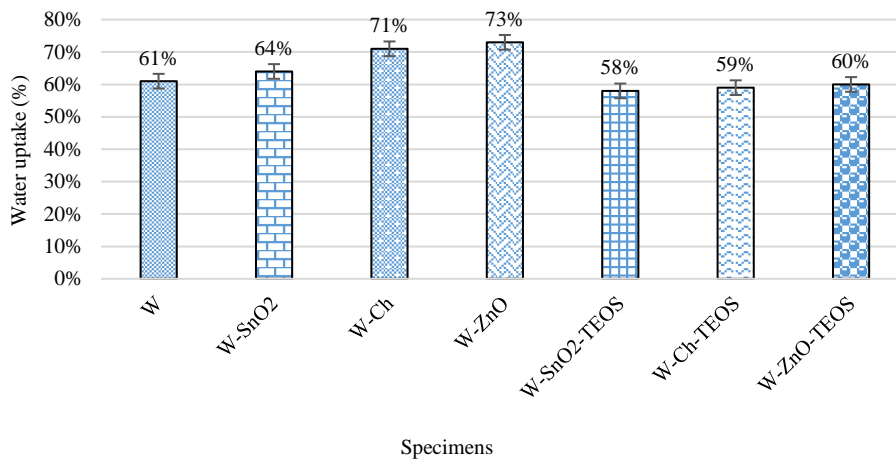


Figure 25. Water absorption percentages of all samples [W (Wood), W-Ch-TEOS (Wood-Chitosan-TEOS), W-ZnO-TEOS (Wood-ZnO-TEOS), and W-SnO₂-TEOS(Wood-SnO₂-TEOS)].

Those wood protection processes can be ranked from best to weakest based on the weight loss observed at different temperature ranges:

1. W-ZnO-TEOS: This process exhibited a significant weight loss at temperatures of 340-375°C, accounting for 62.1% (5.717 mg) of the total weight loss. The second decomposition occurred at 381-439°C, representing 14.4% (1.328 mg) of the weight loss.
2. W-SnO₂-TEOS: This process showed a weight loss of 46.3% (7.050 mg) at temperatures of 301-353°C and 15.4% (2.345 mg) at 431-469°C.
3. W-Ch-TEOS: After silanization with TEOS, this process exhibited a weight loss of 66.4% (8.242 mg) at temperatures of 342-365°C and 18.8% (2.335 mg) at 448-476°C.

3.5. Water uptake (%)

The wood samples were measured by weighing them after being soaked in water for 24 hours and calculated according to formula (2).

$$WA = \left(\frac{w_2 - w_1}{w_1} \right) \times 100 \quad (2)$$

The water absorption amount, WA (%), is calculated using the formula: $WA = ((w_2 - w_1) / w_1) \times 100$, where w_1 is the weight (g) of the test specimen before being soaked in water and w_2 is the weight (g) of the test specimen after being soaked in water. It was observed that the solid wood sample (W) had a water uptake of 61% after being soaked in water for 24 hours, while the samples functionalized with zinc oxide (ZnO), chitosan (Ch), and tin dioxide (SnO₂) nanoparticles exhibited an increase in water uptake values of 64%, 71%, and 73%, respectively, due to the formation of chromophoric carbonyl (C=O, -NO₂, -NO, C=C, -CHO) and carboxyl (R-COOH) groups caused by surface damage (Ramazanoğlu et al., 2022; 2023). The water uptake values after silanization with TEOS were 58%, 59%, and 60%,

respectively (Figure 25). These values are an indicator of increased hydrophobicity.

4. Conclusion

According to SEM and EDX analysis, it was observed that nanoparticles applied by the impregnation method were positioned on the surface by electrostatic force. Changes in surface morphology and color spectra were observed after each functionalization.

According to TGA and DTA analysis results, functionalization has provided the preservation of the lignocellulosic structure by showing less degradation compared to solid wood. However, the hydrophilic lignocellulosic structure has been damaged by Ch, ZnO, and SnO₂ nanoparticles, causing mass loss and the formation of many free radical end groups such as chromophoric carbonyl and carboxyl groups, leaving the structure more hydrophilic and unprotected against environmental conditions. However, the fire resistance has increased after the silanization with TEOS.

Finally, it was observed that the water absorption rate increased when nanoparticles were attached to the surface during the water absorption experiments, indicating the successful attachment of nanoparticles through the impregnation method. Successful results were achieved except for the surface treated with zinc oxide hydrophobized with TEOS. This wood protection approach involves immersion in the chemical solution for functionalization, eliminating the need for additional heating, pressure, or specific conditions, making it a cost-effective method compared to traditional approaches. In future studies, the level of protection can be enhanced by applying different nanoparticles and hydrophobic agents to the lignocellulosic surface.

Acknowledgements

The corresponding author would like to express gratitude to Mr. Muhammed Maraşlı, a Fibrobeton board member, and all Fibrobeton R&D center employees for their support in conducting the color measurement analysis. Additionally, appreciation is extended to Prof. Dr. Serkan Subaşı for providing access to the Duzce University Composite laboratory facilities.

References

- Alfredsen, G., Eikenes, M., Solheim, H., Militz, H., 2004. Screening of chitosan against wood-deteriorating fungi. *Scand. J. Forest Res.*, 19(5): 4-13.
- ASTM-D2244-21, 2021. Standard Practice for Calculation of Color Tolerances and Color Differences from Instrumentally Measured Color Coordinates. *Annual Book of ASTM Standards, USA*.
- Aversa, M., Van Der Voort, A.J., De Heij, W., Tournois, B., Curcio, S., 2011. An Experimental Analysis of Acoustic Drying of Carrots: Evaluation of Heat Transfer Coefficients in Different Drying Conditions. *Drying Technology*, 29(2): 239-244.
- Bantle, M.; Eikevik, T.M., 2011. Parametric Study of High-Intensity Ultrasound in The Atmospheric Freeze Drying of Peas. *Drying Technology*, 29(10): 1230-1239.
- Bulian, F., Graystone J. A., 2009. *Industrial Wood Coatings. Theory and Practice*, First Edition, Elsevier, Amsterdam, pp. 135.
- Carcel, J. A., Garcia-Perez, J.V., Riera, E., Mulet, A., 2011. Improvement of Convective Drying of Carrot by Applying Power Ultrasound Influence of Mass Load Density. *Drying Technology*, 29(2): 174-182.
- Chirkova, J., Anderson, I., Irbe, I., Spince, B., Andersons, B., 2011. Lignins as agents for bio-protection of wood. *Holzforchung* 65(4): 497-502.
- Clausen, P.A. Helle, M., Kärki, P., 2004. Environmental aspects of wood protection and preservation. *Environmental Pollution*, 128 (1):57-64.
- Croitoru, C., Patachia, S., Lunguleasa, A., 2015. A mild method of wood impregnation with biopolymers and resins using 1-ethyl-3-methylimidazolium chloride as carrier. *Chem. Eng. Res. Des.*, 93, 257-268.
- De la Fuente-Blanco, S., De Sarabia, E. R. F., Acosta-Aparicio, V. M., Blanco-Blanco, A., Gallego-Juarez, J.A., 2006. Food Drying Process by Power Ultrasound. *Ultrasonics*, 44(4): 523-527.
- Duan, X., Zhang, M., Li, X., Mujumdar, A.S., 2008. Ultrasonically Enhanced Osmotic Pretreatment of Sea Cucumber Prior to Microwave Freeze Drying. *Drying Technology*, 26(4): 420-426.
- Eikenes, M., Alfredsen, G., Christensen, B., Militz, H., Solheim, H., 2005. Comparison of chitosan with different molecular weights as possible wood preservatives. *J. Wood Sci.*, 51(4): 387-394.
- El-Gamal, R., Nikolaivits, E., Zervakis, G.I., Abdel-Maksoud, G., Topakas, E., Christakopoulos, P., 2016. The use of chitosan in protecting wood artifacts from damage by mold fungi. *Electron. J. Biotechnol.*, 24, 70-78.
- Fan, L. Hu, Z. Wang., J. Chen., 2014. Enhancement of wood properties by multifunctional coatings, *Progress in Organic Coatings*, 77(8):1734-1742.
- Fan, Y. Hu, L., Chen, J., 2013. Multifunctional coatings for wood protection, *Progress in Organic Coatings*, 76(7):1027-1036.
- Floros, J.D., Liang, H.H., 1994. Acoustically Assisted Diffusion Through Membranes and Biomaterials. *Food Technol-Chicago* 48(12): 79-84.
- Garcia, H., Ferreira, R., Petkovic, M., Ferguson, J.L., Leitao, M.C., Gunaratne, H.Q.N., Seddon, K.R., Rebelo, L.P.N., Pereira, C.S., 2010. Dissolution of cork biopolymers in biocompatible ionic liquids, *Green Chem.* 12(3): 367-369.
- Garcia-Perez, J.V., Carcel, J.A.; Riera, E.; Mulet, A., 2009. Influence of The Applied Acoustic Energy on The Drying of Carrots and Lemon Peel. *Drying Technology* 27(2):281-287.
- Garcia-Perez, J.V., Ozuna, C., Ortuno, C., Carcel, J.A., Mulet, A., 2011. Modeling Ultrasonically Assisted Convective Drying of Eggplant. *Drying Technology* 29(13): 1499-1509.
- Griffini, G., Passoni, V., Suriano, R., Levi, M., Turri, S., 2015. Polyurethane coatings based on chemically unmodified fractioned lignin, *ACS Sustain. Chem. Eng.* 3(6): 1145-1154.
- He, Z.B., Yang, F., Yi, S.L., Gao, J.M., 2012. Effect of Ultrasound Pretreatment on Vacuum Drying of Chinese Catalpa Wood. *Drying Technology* 30(15): 1750-1755.
- Herrera, R., Gordobil, O., Llano-Ponte, R., Labidi, J., 2016. Esterified lignin as hydrophobic agent for use on wood products, in: *Proceedings of the COST Action FP1407, 2nd Conference, Innovative Production Technologies and Increased Wood Products Recycling and Reuse*, 29-30 September 2016, Brno, Czech Republic, p. 79.
- Jangam, S.V., 2011. An Overview of Recent Developments and Some R&D Challenges Related to Drying of Foods. *Drying Technology* 29(12): 1343-1357.
- Kim, K.S. Kim, Y.H., Kim, Y.S., 2018. A review of the environmental impacts of wood preservatives. *Environmental Research Letters*, 13, (8):085007.
- Krishnan, R.T., Adhikari, B.S., 2014. Environmental impact of wood preservatives: a review, *Environmental Monitoring and Assessment*, vol. 186, (1): 499-515.
- Laflamme, P., Benhamou, N., Bussières, G., Dessureault, M., 2000. Differential effect of chitosan on root rot fungal pathogens in forest nurseries, *Can. J. Bot.* 77(10): 1460-1468.
- Larnøy, E., Eikenes, M., Militz, H., 2005. Uptake of chitosan based impregnation solutions with varying viscosities in four different European wood species, *Holz Roh-Werkst.* 63(6): 456-462.
- Mothibe, K.J., Zhang, M., Nsor-atindana, J., Wang, Y.C., 2011. Use of Ultrasound Pretreatment In Drying of Fruits: Drying Rates, Quality Attributes, and Shelf Life Extension. *Drying Technology* 29(14):1611-1621.
- Nowrouzi, Z., Mohebbi, B., Younesi, H., 2016. Treatment of fir wood with chito- san and PEG, *J. Forestry Res.* 27(4): 959-966.
- Ojanen J., Kärki, P., 2010. Chemical wood protection: an overview of the history, current state and challenges. *Wood Material Science & Engineering*, 5 (3):137-150.
- Patachia, S., Croitoru, C., Friedrich, C., 2012. Effect of UV exposure on the surface chemistry of wood veneers treated with ionic liquids, *Appl. Surf. Sci.* 258(18): 6723- 6729.
- Ramazanoğlu, D., Mohammed, Z.A., Khalo, I., Maher K., 2022. Aubergine-based Biosorbents for Heavy Metal Extraction. *Bayburt Üniversitesi Fen Bilimleri Dergisi*, 5 (2): 198-205.
- Ramazanoğlu, D., Mohammed, Z.A., Maher, K., 2023. Investigation Usability of Biosorbents Obtained from Orange peels in Heavy Metal Adsorption. *Şırnak Üniversitesi Fen Bilimleri Dergisi*, 3 (2): 1-12.
- Ramazanoğlu, D., Özdemir, F., 2020a. Ahşap Yüzeyde Akıllı Nano Biyomimetik Hidrotermal Lokasyonlama, *Bartın Orman Fakültesi Dergisi*, 22 (2): 447-456.
- Ramazanoğlu, D., Özdemir, F., 2020b. Ön İşlem Olarak Uygulanan Ultrasonik Banyonun Ceviz Kaplamaların Özellikleri Üzerine Etkileri . *Bartın Orman Fakültesi Dergisi*, 22 (2): 479-484.
- Ramazanoğlu, D., Özdemir, F., 2020c. Hidrotermal yaklaşımın lignoselülozik yüzeydeki akıllı nano biyomimetik yansımaları . *Turkish Journal of Forestry*, 21 (3), 324-331
- Ramazanoğlu, D., Özdemir, F., 2020d. Smart nano biomimetic hydrothermal location on wooden surface. *Bartın Orman Fakültesi Dergisi* 22 (2): 447-456
- Ramazanoğlu, D., Özdemir, F., 2021. ZnO-based Nano Biomimetic Smart Artificial Form Located on Lignocellulosic Surface with Hydrothermal Approach. *Kastamonu University Journal of Forestry Faculty*, 21 (1): 12-20.
- Ramazanoğlu, D., Özdemir, F., 2022. Biomimetic surface accumulation on Fagus orientalis. *Appl Nanosci* 12,2421–2428.
- Reddy, M.V. Sunkara, S.B. Raju, K.S. Prasad, V.S.R.K., 2012. Synthesis and Characterization of Chitosan/Titania Nanocomposites, *Journal of Nanomaterials*, vol. 2012, Article ID 849362, 7 pages.

- Schaller, C., Rogez, D., 2007. New approaches in wood coating stabilization, *J. Coat. Technol. Res.* 4(4): 401-409.
- Stasiewicz, M., Fojutowski, A., Kropacz, A., Pernak, J., 2008. 1-Alkoxymethyl-X- dimethylaminopyridinium-base ionic liquids in wood preservation, *Holzforschung* 62(3): 309-317.
- Tanaka, T., Avramidis, S., Shida, S., 2010. A Preliminary Study on Ultrasonic Treatment Effect on Transverse Wood Permeability. *Maderas. Ciencia y Tecnología* 12(1): 3-9.
- Tarleton, E., 1992. The Role of Field-Assisted Techniques in Solid/Liquid Separation. *Filtr Separat* 29(3): 246-238.
- Tarleton, E., Wakeman, R., 1998. *Ultrasound Food Process.* Thomson Science, London, United Kingdom. 193-218
- Wan, P.J., Muanda, M.W., Covey, J.E., 1992. Ultrasonic vs Nonultrasonic Hydrogenation in A Batch Reactor, *Journal of the American Oil Chemists Society* 69(9): 876-879.
- Xu, H., Zhang, M., Duan, X., Mujumdar, A.S., Sun, J., 2009. Effect of Power Ultrasound Pretreatment on Edamame Prior to Freeze Drying. *Drying Technology* 27(2): 186-193.
- Zhou, L., & Fu, Y., 2020. Flame-Retardant Wood Composites Based on Immobilizing with Chitosan/Sodium Phytate/Nano-TiO₂-ZnO Coatings via Layer-by-Layer Self-Assembly. *Coatings*, 10(3): 296. MDPI AG.
- Zhou, W., Sun, F., Pan, K., Tian, G., Jiang, B., Ren, Z., Tian, C. & Fu, H., 2011. Well-Ordered Large-Pore Mesoporous Anatase TiO₂ with Remarkably High Thermal Stability and Improved Crystallinity: Preparation, Characterization, and Photocatalytic Performance. *Advanced Functional Materials*, 21(10): 1922-1930.